A Numerical Investigation on the Bedding Resistance of Laterally Displaced Pipelines

T. Gerlach, M. Achmus, and M. Narten

Institute for Geotechnical Engineering

Leibniz University of Hannover, Germany

Abstract: *The soil resistances in axial and lateral direction strongly affect the behavior of earth-buried district heating pipes under variable operating temperatures. The state of knowledge regarding these resistance forces is summarized, and it is shown that almost no information exists regarding the cyclic effects on lateral soil resistances. However, for the safe design of a district heating network, the forces that soil can exert on the structure due to relative soil-pipe displacements are of particular interest. So, a numerical model has been developed, using the concept of hypoplasticity as an advanced constitutive model for noncohesive, granular materials. Additionally the intergranular strain overlay comes into use, enabling a realistic prediction of soil behavior under cyclic loading. The material model is included using the Abaqus umat interface. Results gained from the finite element model are compared to results from an experimental test with cyclic lateral loading of a pipe. Due to the satisfying agreement, numerous variations on loading device have been done. The investigations give a first insight into the behavior of cyclic laterally loaded district heating pipes.*

Keywords: Abaqus, hypoplasticity, intergranular strain concept, soil-structure-interaction, slave-master-concept, district heating networks, pipelines.

1. Introduction

District heating is a concept where the heat is produced in a centralized location and transported to the customer via pipelines. The heat is taken from combined heat and power, biomass, geothermal heating, heat pumps, or solar heating plants and can be used for space and water heating. Due to the high energy efficiency of district heating with combined heat and power, the supply networks are continually being expanded. In 2006 district heating had a market share of around 14% in the residential building sector of Germany. The connected power capacity was around 52.729MW (AGFW, 2006).

For the design of safe district heating systems, the occuring forces that the soil can exert on the pipeline have to be determined. During the operation of district heating networks, changes of the media temperature lead to periodic varying loading conditions. Hereby, the free movement of the pipe, which tends to elongate and shorten under temperature load, is hindered by the adjacent soil. The resistance of the soil can be divided into axial friction resistance and lateral bedding resistance. Within this paper the focus is set on the latter mentioned. While the bedding resistance under lateral monotonic displacement has already been investigated, the knowledge concerning cyclic influences is limited.

In a research project funded by the German Federal Ministry for Economic Affairs and Energy, the cyclic features of lateral soil resistances on pipes are investigated. Herein, experimental tests and numerical simulations are carried out. This paper firstly outlines the state of knowledge regarding the lateral resistances acting on district heating pipes. Then a numerical model for the calculation of lateral soil resistances under monotonic and cyclic loading is presented. First results of experimental tests are used for calibration and validation of the numerical model. Finally a parametric study on the impact of cyclic displacement amplitude and number of cycles is presented.

2. State of Knowledge

The system under consideration and the denominations are depicted in Figure 1. The problem to be dealt with is to predict the lateral resistance force F_B or the average bedding pressure p_m dependent on the lateral deflection y.

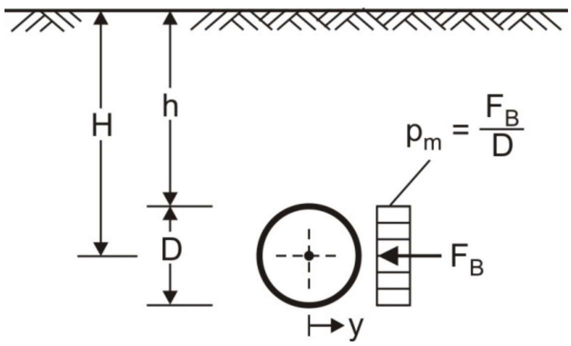

Figure 1. System and denominations for the problem of lateral soil resistance

The first publication on this subject was presented by Audibert and Nyman. They carried out a laboratory test series where the influence of soil density, pipe diameter and embedment ratio was investigated. A detailed description of the test setup can be found in (Audibert, 1975). An air dried, clean medium sand, termed Carver sand, was used for testing. The scope of laboratory investigations included three different diameters, the distinction between loose and dense sand and the variation of cover ratio (depth of cover/pipe diameter). Additionally, one field test was carried out. As a schematic result, Audibert and Nyman pointed out two kinds of failure mechanisms dependent on the embedment depth. This was possible due to a transparent plexiglass window, which made the inspection of the soil movement possible. For a better view, in some tests thin layers of charcoal powder were added. It was found that for shallow burials, less than three times of the pipe's diameter, two wedges are formed. A passive wedge can by observed in front of the pipe (in direction of displacement). Behind the pipe, a smaller, nearly vertical wedge is forming an active zone. With increasing burial depth, the lower bounds of the wedges become steeper and between the two wedges a seperating zone forms, in which no vertical movement of the soil is observed, compare Figure 2a. With further increase of depth, the passive wedge degenerates into a confined zone of soil flow. At this state no disturbance at the surface occurs, as it is illustrated in Figure 2b.

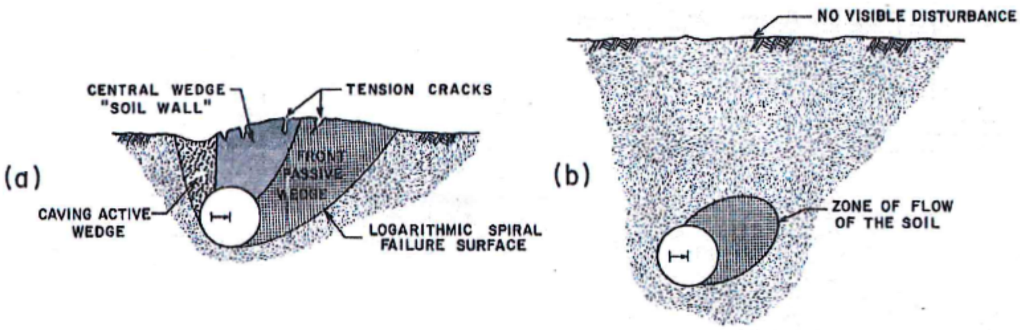

Figure 2. Failure mechanisms according Audibert & Nyman (Audibert, 1977)

Another goal was to find an analytical representation for the soil resistance-displacement relationship. A nonlinear curve which represents the relation of bedding resistance p over displacement y from the initial state to the maximal displacement y_u was found. At y_u, the soil reaction force reaches its maximum value p_u. According to Audibert and Nyman, the normalized bedding resistance $\tilde{p}$ over the normalized displacement $\tilde{y}$ can be approximated by:

$$\tilde{p} = \frac{\tilde{y}}{0.145 + 0.855\,\tilde{y}} \qquad (1)$$

The two normalized parameters are defined as:

$$\tilde{p} = \frac{p}{p_u} \qquad \text{and} \qquad \tilde{y} = \frac{y}{y_u} \qquad (2)$$

So, to predict the bedding resistance for any state of displacement the maximum bedding resistance p_u and the maximum displacement y_u are needed. The maximum of bedding resistance can be obtained from:

$$p_u = \gamma * H * N_u \qquad (3)$$

Herein, γ is the soil unit weight, H the embedment depth and N_u is a bearing capacity factor found by Brinch Hansen (Hansen, 1961). This factor can be taken from a chart, depending on the angle of internal friction and the cover ratio. Audibert and Nyman found a good agreement between their experimental laboratory and field tests carried out by Brinch Hansen. Also, for the derivation of the maximum displacement y_u an approximation was determined. Here, the relation between maximum displacement and depth of embedment (in percent) is plotted over diameter. For a diameter of D = 1 m the maximum displacement y_u is up to 6 % of the depth of embedment H.

With increasing diameter, the ratio of y_u/H is regressive, and a lower limiting value for the ratio y_u/H can be observed. For loose and dense sand, the values were found to be $y_u = 0.015H$ and $y_u = 0.02H$, respectively. This is reported to be in close agreement with the results of Das (Das, 1975), who investigated the subgrade reaction on vertical anchor plates.
Further experimental work was carried out by Trautmann and O' Rourke (Trautmann, 1985). A total of 30 lateral loading tests were performed. The relation between normalized bedding resistance $\tilde{p}$ over normalized displacement $\tilde{y}$ was found similar to Audibert and Nyman, while the bearing capacity factors are much lower.
Achmus (Achmus, 1995) investigated the bedding resistance of laterally displaced pipes numerically. Within his finite element modeling, he used the incremental-elastic material law of Duncan and Chang (Duncan, 1970). Assuming plane strain conditions, the influences of cover ratio, distance to the border of the trench, and pipe diameter were investigated. It is pointed out that the diameter of the pipe obeys a functional relation of the bearing capacity factor. This gives an explanation for the differing values of the bearing capacity factor as determined by Audibert and Nyman, who mainly investigated pipes with diameters of D = 25mm and D = 60mm, and Trautmann and O' Rourke, who used pipes with D = 102mm and D = 324mm.
The calculated bearing capacity factors for different deposit densities, burial depth ratios and nominal pipe diameters are shown in Figure 3.

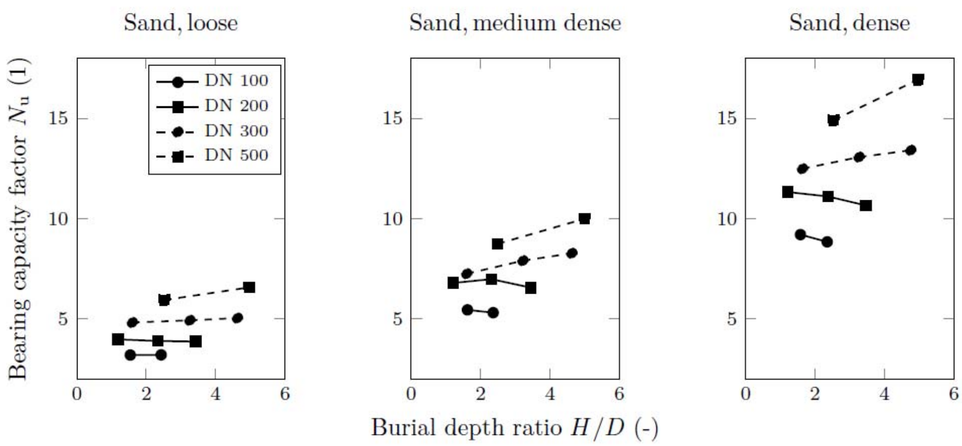

Figure 3. Bearing capacity factors acc. to Achmus

Regarding the development of lateral bedding resistances on pipes with un- and reloading and with repeated (cyclic) loading, the state of knowledge is very limited. It is generally known that foundations or structures in soil under cyclic loading can exhibit an accumulation of displacements. With un- and reloading a hysteresis loop is observed, and the un- and reloading stiffnesses may change with the number of load cycles. However, at the time being, for cyclic lateral displacements of piles an accurate prediction of the bedding resistance is not possible.

3. Experimental Investigations

Experimental tests were carried and shall be used for the calibration and validation of the numerical model. A sketch of the test device is shown in Figure 4. The testing pit has a width of 2.04m, a length of 2.96m and a depth of 1.57m. Two of the walls are made of concrete, while the other two are soldier pile walls, so that the assumption of a stiff enclosure seems appropriate. The sand is poured in layers and compacted with a vibratory device. A deposit density of $D_r = 0.72$ was measured in laboratory and field testing. After the first layer with a height of 0.4m is prepared, a concrete filled steel tube with an outer diameter of D = 0.27m is placed on top.

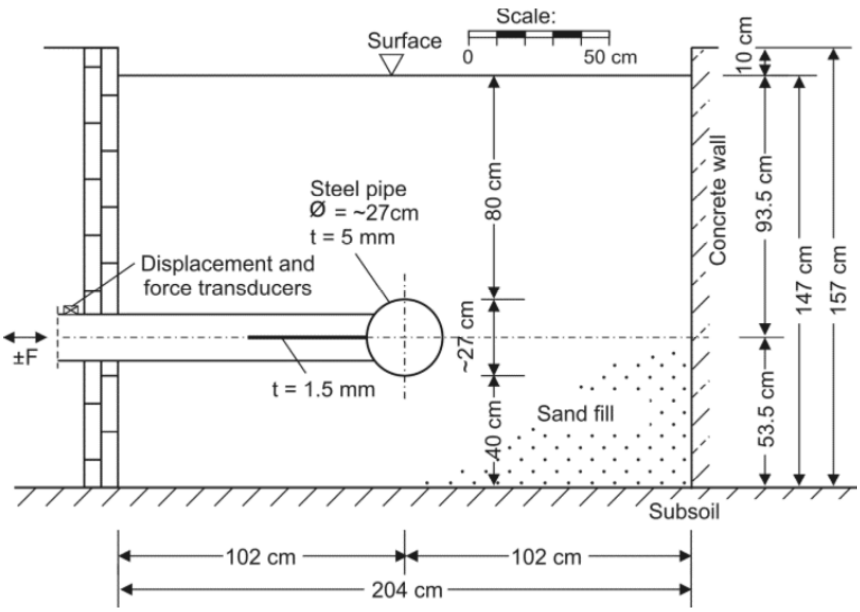

Figure 4. Sketch of the testing device

The load equipment is orthogonally welded to the pipe. It consists of a hydraulic press which is connected to the pipe by a steel tube, strengthened by two flanges. In the second layer, four transducers are installed to measure the occurring earth pressures. Sand is then filled up to a cover ratio of 3 and densified. Afterwards, the measuring instruments are calibrated to zero, followed by the displacement-controlled loading of the pipe. The experimental result can be seen in Figure 5. The peak strength has been surpassed within the primary displacement to y = 4.5cm. Afterwards, a total of 40 displacement cycles with a constant amplitude of 1.25cm are applied. The mean displacement is increased in steps of 0.5cm from 3.75cm to 5.25cm at intervals of ten cycles so that the first ten cycles are in the range between 2.5cm and 5.0cm. Figure 5 shows that the bedding pressure at maximum displacement decreases only slightly in each cyclic loading phase. The (negative) maximum bedding pressure on the left side of the pipe first increases with the number of load cycles, until almost the same value as on the right side is reached. In subsequent cycles, the maximum bedding pressure remains constant or increases slightly, as it does on the right side of the pipe.

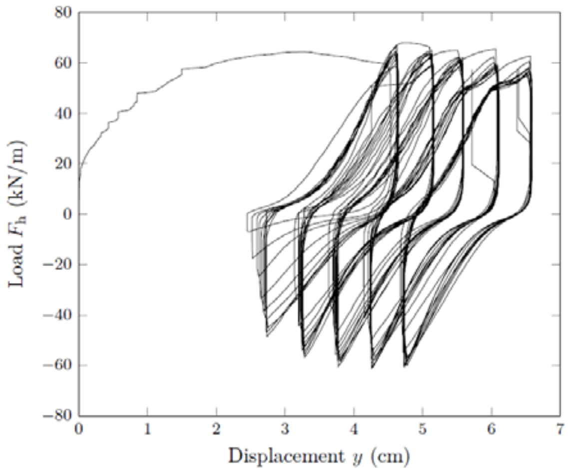

Figure 5. Force-displacement-curve from experimental test

4. Numerical Investigations

The primary loading and the first load level were computed using Abaqus, assuming plane strain conditions. However, it must be taken into account that the loading tube might hinder the free movement of soil around the pipe. It is questionable whether the length of the pit is long enough to avoid an influence of the vertical walls parallel to the loading tube. This should be investigated in the future using a three dimensional model. Nevertheless, plane strain conditions are deemed appropriate for the given problem as the main influences on the bedding resistance, geometrically and materially, can be investigated. For the developed model, the element CPE8 comes into use. This 8-node element is full integrated (9 Gaussian points) and uses quadratic shape functions. In contrast to elements with first-order (linear) interpolation, these second-order elements are capable of representing all possible linear strain fields. Additionally the shape approximation of curved structures is much better, because the line between two nodes is not necessarily straight. Thus, a more accurate solution may be obtained with fewer elements in contrast to first-order elements. Within the soil layers a size bias is used so that the size of the element is increasing with the distance from the pipe. Hence, the region near the pipe can be discretized finer than the elements at a larger distance where the mesh density can usually be reduced because of lower stress gradients. The pipe is assumed to be very stiff and thus not deformable, allowing it to be approximated by an analytical circular surface. This can be done easily in Abaqus and comes with a few advantages. The curved geometry of a pipe can be modeled exactly with analytical surfaces, using curved line segments. The result is a smoother surface description, which can reduce contact noise and provide for a better geometry approximation. The reference node, whose motion governs the motion of the surface, is used to apply a prescribed pipe displacement. To take into account the field installation process four geostatic load steps are computed, where the soil gets activated in layers, so that the underlying soil would be prestressed.

A relative displacement between the pipe and the surrounding soil occurs under lateral pipe displacement. To enable the possibility of relative slipping within the finite element model, a contact condition is defined. For the contact with an analytical rigid surface, the node to surface option must be used. In this case, the contact conditions are established such that each slave node interacts with a point of projection on the master surface. The frictional contact is established using the simple friction law according to Coulomb. The classical Couloumb's friction law considers the stick-slip phenomenon, which describes the transition between stick and slip states, depending on the magnitude of applied contact pressure. In contrast, Abaqus employs a nonlocal friction model, where the full mobilization of the limit frictional stress is dependent both on the relative displacement between the pipe and soil as well as on the friction coefficient. The relative displacement after which the maximum shear stress is reached, is denoted as the critical shear displacement, limiting the elastic range. If the critical shear displacement is exceeded, the surfaces slide over each other and the friction changes from static friction to kinematic friction. For the calculations a critical shear displacement of s_{crit} = 1.0mm and a coefficient of friction of $\mu = 0.42$ (corresponding to two third of the angle of internal friction) has been chosen for the soil-pipe as well as for the soil-wall interaction.

The constitutive law of hypoplasticity is used to describe the soil behaviour. An implementation of hypoplasticity as an Abaqus compatible user material (umat) is employed (Gudehus, 2008). The hypoplastic material law is a rate-type model which accounts for the complex non-linear soil behavior by just one (rather sophisticated) tensorial equation. In its original form, the hypoplastic material law needs eight parameters (von Wolfferdorff, 1996). It uses the stress state and the void ratio of a non-cohesive material as state variables and accounts for stress-dependence of soil stiffness and soil strength, thereby reflecting contractancy or dilatancy of soils under shearing in a realistic manner. The material law in the original form was found to overestimate the accumulation of soil deformations under cyclic loading.

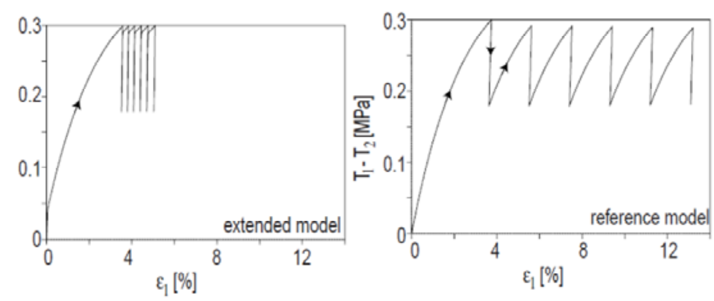

Figure 6. Cyclic stress-strain relation: Hypoplastic model without (right) and with (left) intergranular strain (Niemunis, 1997)

Therefore, the intergranular strain concept was developed, which cares for a realistic simulation of the behavior under cyclic loads (see Figure 6). However, another five parameters are necessary to define the behavior with consideration of intergranular strain (Niemunis, 1997). The needed input parameters for the extended hypoplastic model were determined through laboratory testing, including cyclic triaxial tests. They have been slightly adjusted to fit better with the experiment. The used parameters are summarized in Table 1.

Table 1. Input parameters for the hypoplastic model with intergranular strain

φ_c	h_s	n	e_{d0}	e_{c0}	e_{i0}	α	β	m_R	m_T	R	β_r	χ
(°)	(MPa)	(-)	(-)	(-)	(-)	(-)	(-)	(-)	(-)	(-)	(-)	(-)
29.0	4000	0.29	0.443	0.898	1.08	0.1	2.0	6.0	3.0	0.00008	0.8	5.0

Before the backcalculation of the experimental data was done, the developed model was checked for accuracy. Since the quality of mesh discretization has an important impact on the calculated results, a study on mesh fineness was performed. However, a more accurate calculation is associated with an increase in calculation time. The chosen mesh is displayed in Figure 7, for which the element surfaces along the pipe's circumference have a length of 1.4cm. Taking into account the quadratic shape functions, the pipe discretization angle is 2.81°.

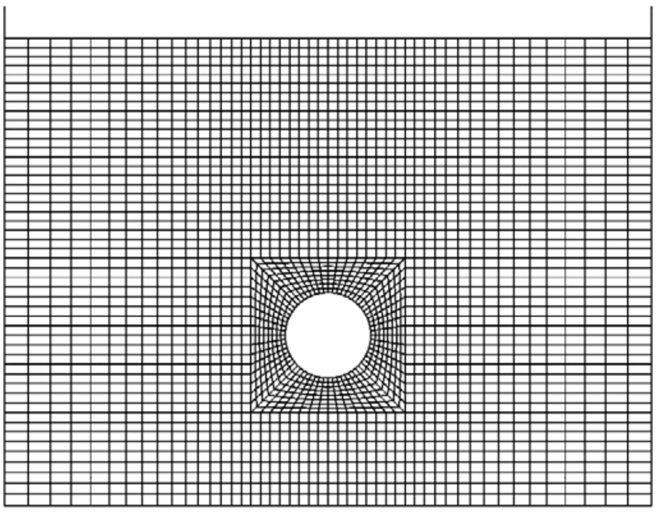

Figure 7. Finite element mesh used for the calculations

As can be seen in Figure 8, the numerical results are in a fair overall agreement with the experimental results. The numerical model seems thus capable to properly describe the main features of the system behavior.

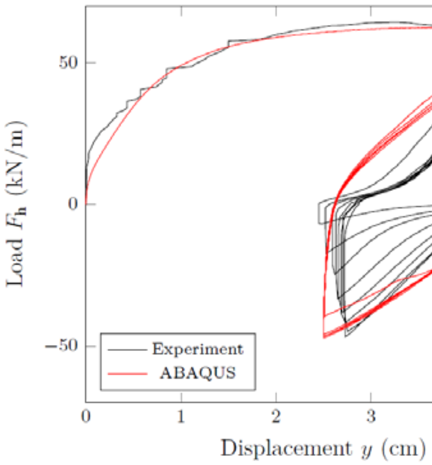

Figure 8. Comparison between experimental and numerical results

To get a better insight on the impacts of cyclic pipe displacement on the occurring bedding resistance, a parametric study of the loading was performed. Based on the resulting force-displacement curve of the presented experimental test, a mean displacement of y = 0.6cm was selected to investigate the behavior of cyclic loading prior to reaching the peak strength. The amplitude of displacement was chosen to be 0.25cm, 0.50cm, 0.75cm, and 1.25cm. A number of 16 load cycles were applied for each displacement amplitude. The results of the study are plotted in Figure 9. Herein, the reduction factor denotes the reaction force at the peak of each cycle normalized w.r.t. the reaction force after the primary loading.

As can be seen, for all amplitudes, the reaction force decreases by about 15% after the first reloading cycle. For the smallest amplitude, the reaction force reaches a constant value after the second cycle. For greater amplitudes, the degradation occurs slower. Note that the given values for the normalized reaction force are related to the maximum displacement of each calculation and not to peak strength. So the degradation of the peak strength may differ from these values.

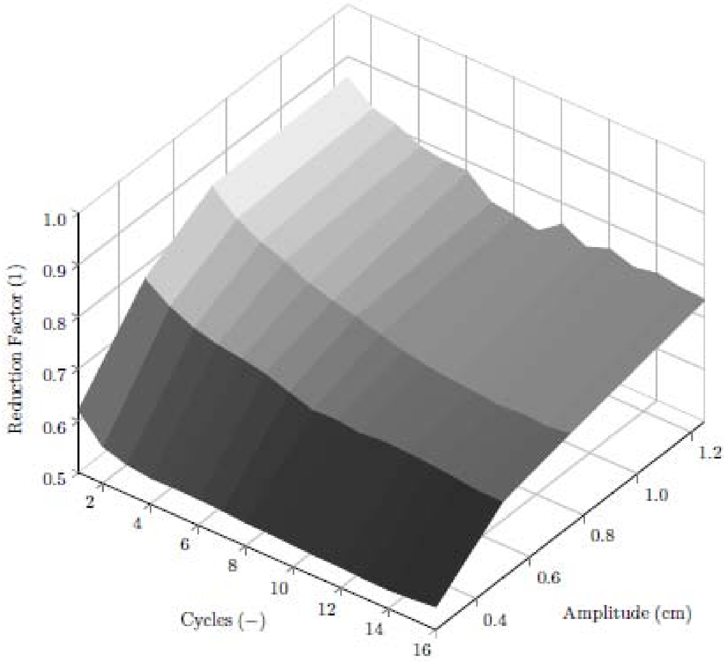

Figure 9. Reduction factor for varying amplitude of displacement and cycle number

5. Conclusion

A numerical model with an advanced material law was developed, which predicts the behavior of a cyclic laterally loaded pipe buried in sand. Results derived with this model are compared to results from an experimental test in which cyclic lateral displacements were applied on a pipe section. Good agreement regarding the basic features of the system behavior was observed. This shows that the model is capable of reflecting the main features of the complex system behavior. A parametric study was carried out, showing the impacts of displacement amplitude and number of cycles. Herein the amplitude could be identified for being more influencing on the pipes reaction force. Nevertheless, more research is needed for a more accurate prediction of the pipe behavior in operation and with that to reach an optimized design of such pipelines.

6. References:

1. Achmus, Martin: Zur Berechnung der Beanspruchungen und Verschiebungen erdverlegter Fernwärmeleitungen, Universität Hannover, Ph.D. thesis, 1995 (in German).
2. Arbeitsgemeinschaft für Wärme und Heizkraftwirtschaft - AGFW - e.V., Branchenreport, 2006 (in German).
3. Audibert, Jean M. ; Nyman, Kenneth J.: Coefficients of subgrade reaction for the design of buried piping. In: Structural Design of Nuclear Plant Facilities ASCE, S. 109–141, 1975.
4. Audibert, Jean M. ; Nyman, Kenneth J.: Soil restraint against horizontal motion of pipes. In: Journal of the Geotechnical Engineering Division 103, Nr. 10, S. 1119–1142, 1977.
5. Das, Braja M. ; Seeley, Gerald R.: Load-displacement relationship for vertical anchor plates. In: Journal of Geotechnical and Geoenvironmental Engineering 101, Nr. ASCE 11402 Proceeding, 1975
6. Duncan, James M. ; Chang, Chin-Yung: Nonlinear analysis of stress and strain in soils. In: Journal of the Soil Mechanics and Foundations Division 96, Nr. 5, S. 1629–1653, 1970.
7. G. Gudehus, A. Amorosi, A. Gens, I. Herle, D. Kolymbas, D. Mašín, D. Muir Wood, R. Nova, A. Niemunis, M. Pastor, C. Tamagnini, and G. Viggiani. The soilmodels.info project. International Journal for Numerical and Analytical Methods in Geomechanics, 32(12):1571-1572, 2008.
8. Hansen, J B. ; Christensen, NH: The Ultimate Resistance of Rigid Piles Against Transversal Forces; Model Tests with Tranversally Loaded Rigid Piles in Sand. Geoteknisk Institut, 1961.
9. Niemunis, A ; Herle, I: Hypoplastic model for cohesionless soils with elastic strain range. In: Mechanics of Cohesive-frictional Materials 2, Nr. 4, S. 279–299, 1997.
10. Trautmann, Charles H. ; O'Rourke, Thomas D.: Lateral force-displacement response of buried pipe. In: Journal of Geotechnical Engineering 111, Nr. 9, S. 1077–1092, 1985.
11. Wolffersdorff, P-A von: A hypoplastic relation for granular materials with a predefined limit state surface. In: Mechanics of Cohesive-frictional Materials 1, Nr. 3, S. 251–271, 1996.